Microstructure, localized Cu^{2+} spins, and transport properties of $Bi_2Sr_2Ca_{1-x}Y_xCu_2O_{8+\delta}$

Xu Gaojie
Structure Research Laboratory, University of Science and Technology of China, Hefei, Anhui, 230026, People's Republic of China and Department of Astronomy and Applied Physics, University of Science and Technology of China, Hefei, Anhui 230026, People's Republic of China

Pu Qirong and Ding Zejun
Department of Astronomy and Applied Physics, University of Science and Technology of China, Hefei, Anhui 230026, People's Republic of China

Yang Li and Zhang Yuheng
Structure Research Laboratory, University of Science and Technology of China, Hefei, Anhui, 230026, People's Republic of China

(Received 28 January 2000; revised manuscript received 17 May 2000)

The microstructure, charge transport, and spin dynamics of polycrystalline samples $Bi_2Sr_2Ca_{1-x}Y_xCu_2O_{8+\delta}$ have been studied by x-ray diffraction, electron diffraction, resistivity, thermoelectric power (TEP), and electron spin resonance. It is found that Y^{3+} doping causes a tetragonal-orthorhombic structural transition at $x=0.5$ and leads to the superstructural modulation wavelength changing from $q_b=4.8b$ to $q_b=3.85b$ as x increases from 0 to 1. The enhancement of the structural distortion causes an increase of the fraction of localized Cu^{2+} spins. Resistivity and TEP measurements show anomalies around $x=0.6$, which are interpreted in terms of the spin correlation. The relation of crystal microstructure, localized Cu^{2+} spins, and charge transport is analyzed and discussed based on the experimental results.

I. INTRODUCTION

Investigations of the properties had revealed a common characteristic of many oxide high-T_c superconductors; i.e., they have a CuO_2 plane in their structure. Within the range of lower carrier density, the localized Cu^{2+} spins are correlated antiferromagnetically in the CuO_2 plane. Shirane and co-workers[1] found that the long-range correlation of Cu^{2+} spins exists even in the normal state of superconducting samples. Obviously, a systematic study of the spin dynamics of the bulk Cu^{2+} spin system is important, because this study can reveal the basic elements and mechanisms of the insulator-to-metal transition. Electron spin resonance (ESR) measurements are effective for determining the localized Cu^{2+} spin character. Information is obtained on the g value from the resonance field, on the spin relaxation rate $\Gamma_{\sigma L}$ to the lattice from the signal width, and on the susceptibility from the integrated intensity of the absorption signal. For Bi-based superconductors with complicated incommensurate modulation structure, the ESR method should be more useful for studying the dependence of the localization of Cu^{2+} spins on the microstructural characteristics.

On the other hand, extensive studies have demonstrated that the normal-state transport properties of oxide superconductors are unusual, and systematic studies of them are essential to understand the mechanism of high-temperature superconductivity. Since cuprate superconductors are based on an antiferromagnetic background, it is easy to think that the magnetic interaction may influence the normal-state properties. In fact, it has already been suggested[2,3] that the linear temperature dependence of resistivity is caused by spin fluctuation scattering. Up until now, however, how the spin scattering influences thermoelectric power (TEP) or Hall coefficient (R_H) has been unclear. Zhou and Goodenough[4] have investigated systematically the TEP of copper oxides with single CuO_2 sheets and found that the doping of magnetic ion at non-CuO_2 sheets has little influence on the TEP. Nevertheless, a comparison of the transport properties between double-doped $La_{1.85-x}Sr_{0.15+x}Cu_{1-x}Fe_xO_4$ and $La_{1.85-x}Sr_{0.15+x}Cu_{1-x}Ga_xO_4$ systems[5] demonstrates that Fe doping leads to a broad peak in $S(T)$-T curves shifting up to high temperature, while Ga doping does not influence the broad peak. It is suggested that magnetic scattering plays an important role in charge transport in the Fe-doped system.

Previously, there have been many reports on the structure and transport properties of the Bi2212 system,[6–11] but few reports were contributed to the relationship between the microstructure and the physical properties, as well as the relation between transport properties and spin correlation. In this paper, we systematically investigate the crystal microstructure, charge transport properties, and the spin dynamics of the $Bi_2Sr_2Ca_{1-x}Y_xCu_2O_{8-\delta}$ system.

II. EXPERIMENT

The polycrystalline $Bi_2Sr_2Ca_{1-x}Y_xCu_2O_{8-\delta}$ samples with $0\leqslant x\leqslant 1.0$ were prepared using the solid-state reaction method. The detailed synthesized procedures are similar to that reported previously.[12] The structure of these samples was characterized by x-ray diffraction (XRD) and electron diffraction (ED). The XRD analysis was carried out by a Rigaku-D/max-γA diffractometer using high-intensity Cu $K\alpha$ radiation. The lattice parameters were determined from the d values of XRD peaks by a standard least-squares re-

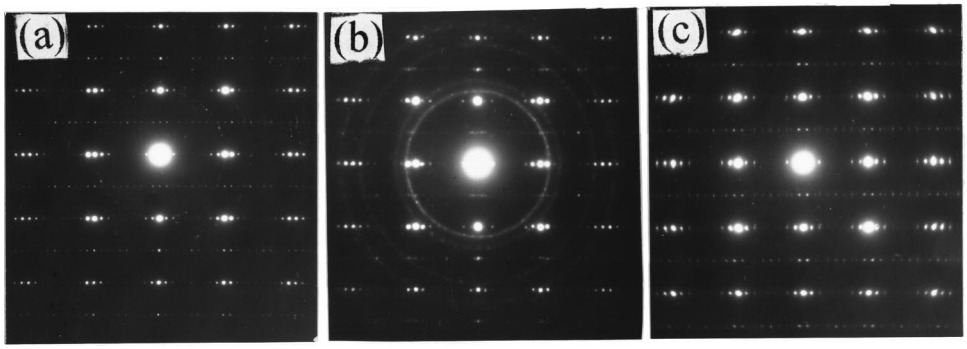

FIG. 1. (a)–(c) [001] zone electron-diffraction patterns of samples $Bi_2Sr_2Ca_{1-x}Y_xCu_2O_{8-\delta}$ (a) $x=0$, (b) $x=0.6$, and (c) $x=1.0$.

finement method. The ED patterns were obtained using an H-800 transmission-electron microscopy. Resistivity as a function of temperature for all the samples was measured using a standard four-probe method in a closed-cycle helium cryostat. The TEP of the samples was measured by a differential method. The temperature at the two ends of the measured sample was controlled automatically within a precision of 0.01 K. The emf of the sample was indicated by a Keithley 181 nanovolmeter with an error less than 0.2 μV. The electron spin resonance (ESR) experiments were carried out at 100 K by a Bruker (ER-200D-SRC) reflection *x*-band-type spectrometer. The frequency counter and magnetic field were measured using a frequency counter and a proton NMR gaussmeter, respectively.

III. RESULTS

XRD patterns show that all the samples are single Bi2212 phase. Table I gives the lattice parameters *a*, *b*, and *c* for $Bi_2Sr_2Ca_{1-x}Y_xCu_2O_{8-\delta}$ samples. As the Y content *x* increases from 0 to 1.0, the parameter *c* decreases monotonously from 30.883 to 30.216 Å, while the *a* increases from 5.4072 to 5.4503 Å. A structural transition from tetragonal to orthorhombic takes place at $x=0.5$ for Ca replaced by Y (see the value of *b*-*a* in Table I). The evidence for this transition can also be obtained from the splitting of the (200) peak for the $x=1.0$ sample. These results are in good agreement with previous reports.[10,13]

Figures 1(a)–1(c) exhibit the electron-diffraction patterns of the [001] zone for samples $Bi_2Sr_2Ca_{1-x}Y_xCu_2O_{8-\delta}$ with $x=0$, 0.6, and 1.0, which appear in most of the observed grains. Similar satellite diffraction spots can be seen in every ED patterns. Previous studies have clarified that Bi-based superconductors (Bi2201, Bi2212) possess complicated incommensurate modulation structure, the supercell of which for the undoped samples is monoclinic (namely, Bi-type modulation).[14,15] Elemental substitution or a change of oxygen content could influence the characteristics of the superstructural modulation. For example, aliovalent cation or equivalent cation substitutions for Sr or Cu of the Bi2201 system can enhance the Bi-type modulation, while Pb doping in Bi_2O_2 layers can relax the Bi-type modulation structure in both the Bi2201 and Bi2212 systems and even lead to the Bi-type modulation disappearing at high doping level. Obviously, the satellite diffraction spots observed in Fig. 1 originate from monoclinic superstructural modulation. The Bi-type incommensurate modulation wavelength (q_b) for the samples with $x=0$, 0.4, 0.6, 0.8, and 1.0 is also given in Table I. Y doping enhances the Bi-type superstructural modulation and leads to a zigzag atomic chain along *c* direction.

TABLE I. Lattice parameters *a*, *b*, and *c* and the discrepancy of *a* and *b* (*b*-*a*), the incommensurate modulation wavelength (q_b) for $Bi_2Sr_2Ca_{1-x}Y_xCu_2O_{8-\delta}$ samples.

Y content *x*	*a* (Å)	*b* (Å)	*c* (Å)	*b*-*a* (Å)	q_b
$x=0$	5.4072	5.4072	30.883	0	4.8*b*
$x=0.2$	5.4187	5.4187	30.714	0	
$x=0.4$	5.4262	5.4262	30.572	0	4.4*b*
$x=0.5$	5.4293	5.4376	30.492	0.0083	
$x=0.6$	5.4335	5.4476	30.421	0.0141	4.2*b*
$x=0.8$	5.4432	5.4593	30.318	0.0161	4.0*b*
$x=1$	5.4503	5.4688	30.216	0.0185	3.85*b*

Figure 2 shows the temperature dependence of resistivity for the samples $Bi_2Sr_2Ca_{1-x}Y_xCu_2O_{8-\delta}$ ($0\leqslant x\leqslant 1.0$). Although all the samples exhibit the ideal 2212 single phase, the superconductivity and charge-transport properties reflected in Fig. 2 are noticeably different. Samples at a low doped level ($x\leqslant 0.3$) all show a higher superconducting transition temperature ($T_c\geqslant 89$ K), and the critical temperature reaches a maximum of about 93 K for the $x=0.1$ sample. The T_c decrease rapidly with increasing *x* as the Y content $x\geqslant 0.4$. No superconductivity was detected down to the lowest measurement temperature (11 K) for the sample with *x*

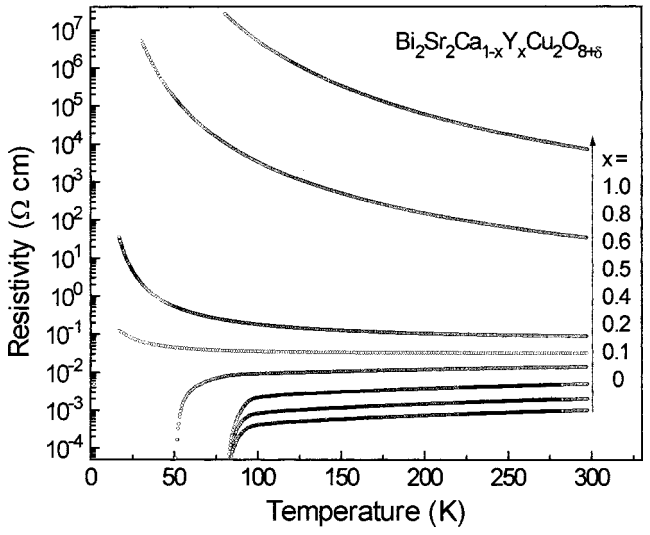

FIG. 2. Temperature dependence of the resistivity for samples $Bi_2Sr_2Ca_{1-x}Y_xCu_2O_{8-\delta}$ ($0\leqslant x\leqslant 1.0$).

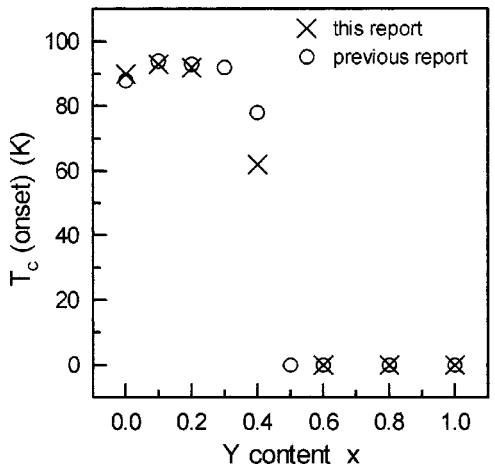

FIG. 3. The variation of the superconducting transition onset temperature (T_c^{onset}) of $Bi_2Sr_2Ca_{1-x}Y_xCu_2O_{8-\delta}$ as a function of Y content x. ×, this report; ○ a previous report by Kakihana *et al.* (Ref. 13).

$\geqslant 0.5$. Figure 3 shows T_c (onset) for the $x=0-0.4$ samples. The relation between T_c and x given here is similar to what had been reported earlier.[10,13,16]

From Fig. 2 one can also find that the temperature coefficient $d\rho/dT$ for the samples with $x\leqslant 0.4$ is positive, indicating metallic conduction. The samples with $x\geqslant 0.5$ show an semiconducting behavior, and the system has transformed from a metal to a semiconductor with $x>0.5$. Now let us turn our attention to the change of the room-temperature resistivity ρ_{300}. For $x\leqslant 0.5$ samples, the ρ_{300} only varies within one to two orders of magnitude. While for the samples with $x>0.5$ the ρ_{300} increases quickly, and the ρ_{300} for $x=1.0$ sample is five orders of magnitude larger than that of $x=0.6$ sample; see Fig. 4. A sharp change in ρ_{300} occurs around $x=0.6$.

Figure 5 displays the TEP as a function of temperature for the samples $Bi_2Sr_2Ca_{1-x}Y_xCu_2O_{8-\delta}$ $(0\leqslant x\leqslant 1.0)$. The $S(T)$ value increases progressively with increasing Y content x. The $x=0$ sample has negative values in the TEP over the whole measured temperature region, while the samples with $x\geqslant 0.1$ all show positive values. For the superconducting samples in the high-temperature region, S increases with decreasing temperature almost linearly, then passes through a

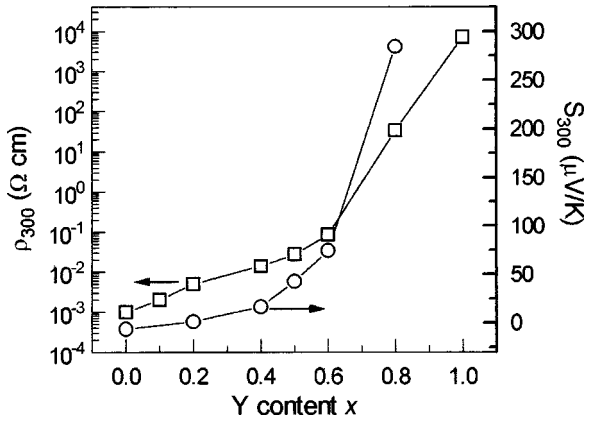

FIG. 4. Room-temperature resistivity (ρ_{300}) and thermoelectric power (S_{300}) as a function of Y content x.

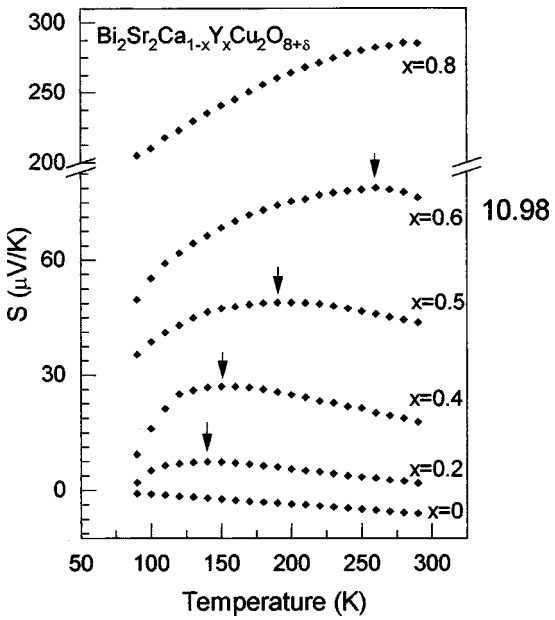

FIG. 5. Temperature dependence of the thermoelectric power of $Bi_2Sr_2Ca_{1-x}Y_xCu_2O_{8-\delta}$ $(0\leqslant x\leqslant 1.0)$.

maximum, and around T_c falls sharply. All the samples, except for $x\geqslant 0.8$ samples, show a broad peak in the $S(T)$-T curve, and the temperature (T_m) corresponding to the peak increases with increasing x. The T_m is 90, 130, 150, 200, and 260 K, respectively, for the samples with $x=0$, 0.2 0.4, 0.5, and 0.6. For $x\geqslant 0.8$ samples, the T_m is greater than 300 K, and the $S(T)$-T curve shows a positive slope in the whole measured temperature region.

The room-temperature TEP (S_{300}) for these samples is also given in Fig. 4. One can find that the variation of S_{300} and ρ_{300} with Y content x has a striking similarity. A large change in S_{300} is also found around $x=0.6$, indicating that similar factors influencing ρ_{300} and S_{300} exist.

The ESR signals at 100 K for the samples $Bi_2Sr_2Ca_{1-x}Y_xCu_2O_{8-\delta}$ $(0\leqslant x\leqslant 1.0)$ are shown in Fig. 6. The g factor corresponding to these lines is approximately 2.1, indicating the dominance of Cu^{2+} spins. In previous ESR investigations, some authors attributed the ESR signal in 0.3–0.35 T range to a small amount of Cu^{2+}-based impurities,[17,18] but Ishida and co-workers[19] found that the ESR signal coming from localized Cu^{2+} spins reproduced the intrinsic susceptibility of the high-T_c superconducting phase. We believed that the argument of Ishida *et al.* is reasonable, because no impurity appears in our samples. From Fig. 6 one can see that the relative intensity of the EPR line increases rapidly as $x\geqslant 0.6$, which indicates a striking increase of the fraction of localized Cu^{2+} spins with Y doping.

IV. DISCUSSION

From the experimental results described above, it is apparent that the substitution of Y for Ca causes a large change in the lattice parameters. A tetragonal-orthorhombic (T-O) structural transition takes place at $x=0.5$. This T-O transition implies the reduction of symmetry and the enhancement of structural distortion. ED patterns show that Y doping intensifies the Bi-type incommensurate modulation, which can be

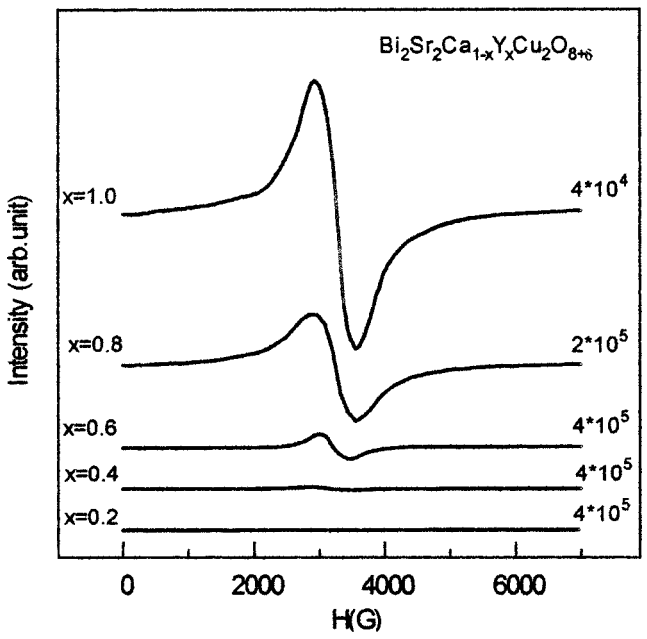

FIG. 6. ESR spectra at 100 K of the $Bi_2Sr_2Ca_{1-x}Y_xCu_2O_{8-\delta}$ samples.

understood in the framework of extra oxygen model[20] and crystal misfit model.[21,22] It has been realized that the modulation structure of Bi-based superconductors originates from the periodic arrangement of Bi-concentrated bands in Bi_2O_2 layers, and the arrangement is caused by the lattice mismatch between Bi_2O_2 layers and perovskite blocks. The extra oxygen model proposed by Zandbergen *et al.*[20] suggested that the periodic intercalation of the extra oxygen atoms in Bi_2O_2 layers was the origin of Bi-concentrated band superstructural modulation and the extra oxygen is brought by the partial substitution of Bi^{5+} instead of Bi^{3+}. Y^{3+} replacing Ca^{2+} in the Y-doped Bi2212 system introduces extra oxygen into Bi_2O_2 layers, thus leading to the incommensurate modulation wavelength decrease. Mao *et al.*[21] and Amelinckx and Van Tendeloo[22] argued that the real driving force of the Bi-concentrated band superstructural modulation was crystal misfit between Bi_2O_2 layers and perovskite blocks, and the presence of extra oxygen atoms in the Bi_2O_2 layers can be regarded as a consequence caused by the crystal misfit. Obviously, the crystal misfit model is also effective in explaining our ED patterns, because of strong structural changes taking place with the substitution of Y^{3+} for Ca^{2+}. For the above two models, the extra oxygen model is successful in interpreting the change of modulation structure of the system with aliovalent ion substitution, such as $Bi_2Sr_{2-x}La_xCuO_y$, $Bi_{2-x}Pb_xSr_2CuO_y$, and $Bi_2Sr_2Cu_{1-x}Fe_xO_y$ systems.[23–25] However, it cannot well account for the variation of the modulation wavelength for equivalent ion substitution, such as Ba^{2+} replacing Sr^{2+} or Zn^{2+} replacing Cu^{2+} in Bi2201 systems, while all these experimental results can be well understood according to the crystal misfit model. So it is suggested that the change of incommensurate superstructural modulation in above Y-doped Bi2212 system originates from the crystal misfit between Bi_2O_2 layers and perovskite blocks along the *b* axis.

It is demonstrated that aliovalent ion substitution causes a change in the distribution of charge between different atomic layers.[26,27] Although some extra oxygen is introduced into Bi_2O_2 layers with the substitution of trivalent Y^{3+} for Ca^{2+}, the amount of oxygen uptake is insufficient to balance the extra charge introduced by Y^{3+}.[28,29] Therefore, Y doping decreases the carrier concentration and leads the system into the underdoped region. The superconductivity disappears as $x \geqslant 0.5$. Fujita and Tomita[30] investigated the structural, magnetic, and superconducting phase diagram of the Y-doped Bi2212 system and found that an antiferromagnetic phase appears under low temperature as $x \geqslant 0.5$ and the T_N increases gradually with increasing Y content. This phase diagram is similar to those of other series of oxides, such as La214 and Y123 systems. The anomaly of ρ_{300} and S_{300} around $x = 0.6$ in the $Bi_2Sr_2Ca_{1-x}Y_xCu_2O_{8-\delta}$ system can be interpreted in terms of this magnetic transition.

It is known that the charge carrier concentration of $0.15 \leqslant x \leqslant 0.20$ per Cu in a CuO_2 sheet appears to give the maximum T_c in all cuprate superconductors and an additional feature influencing T_c is the $(180° - \phi)$Cu-O-Cu bond angle with a CuO_2 sheet. The structural distortion (modulation structure and T-O transition) in the $Bi_2Sr_2Ca_{1-x}Y_xCu_2O_{8-\delta}$ system buckles the Cu-O-Cu bond angle from 180° to $(180° - \phi)$ to relieve the compressive stress on the CuO_2 sheets induced by a mismatch between Bi_2O_2 layers and perovskite blocks. The rapid decrease of T_c in Fig. 3 may be induced by the cooperation of the above two factors, i.e., the change of carrier concentration and the structural distortion.

From ESR results it is found that the relative intensity of ESR lines increases rapidly as $x \geqslant 0.6$, which means that the fraction of localized Cu^{2+} spins increases strikingly with the increase in Y content. This also implies the freezing of spin fluctuations and the concomitant localization of the charge carriers. One knows that the phase diagram of the $La_{2-x}Sr_xCuO_4$ system is similar to that of the Y-doped Bi2212 system. However, we could not observe an ESR signal in the underdoped region of the $La_{2-x}Sr_xCuO_4$ system. Comparing the microstructures between the two systems, one can easily find that the $Bi_2Sr_2Ca_{1-x}Y_xCu_2O_{8-\delta}$ system possesses a complicated incommensurate modulation, while the $La_{2-x}Sr_xCuO_4$ system does not exhibit any modulation characteristic. Y doping not only leads to a T-O structural transition, but also intensifies incommensurate superstructural modulation. The strong modulation wave inevitably causes Cu-atom position to deviate from the *a*-*c* plane, hence enhancing the distortion of the CuO_6 octahedron, especially as $x \geqslant 0.6$. The strongly structural distortion hinders the spin correlation and leads to localized Cu^{2+} spins. The Cu3*d* electrons change from a partially delocalized to a localized state. This localization of Cu3*d* electrons induced by the structural distortion causes the metal-insulator transition of the $Bi_2Sr_2Ca_{1-x}Y_xCu_2O_{8-\delta}$ system.

Kochelaev *et al.* have investigated the spin dynamics of $La_{1.925}Sr_{0.075}CuO_4$ and proposed a three-spin polaron (TSP) model [consisting of two Cu^{2+} ions and one *p* hole ($S = 1/2$)].[31] Our experimental results can also be interpreted using this model; i.e., the formation of TSP favors the localization of Cu3*d* electrons and expedites the decrease of the effective carrier concentration. However, by analyzing the ESR experimental results, we find that the ESR spectrum is much narrower than that obtained in $La_{1.925}Sr_{0.075}CuO_4$ by Kochelaev *et al.* and the ESR signal is a temperature depen-

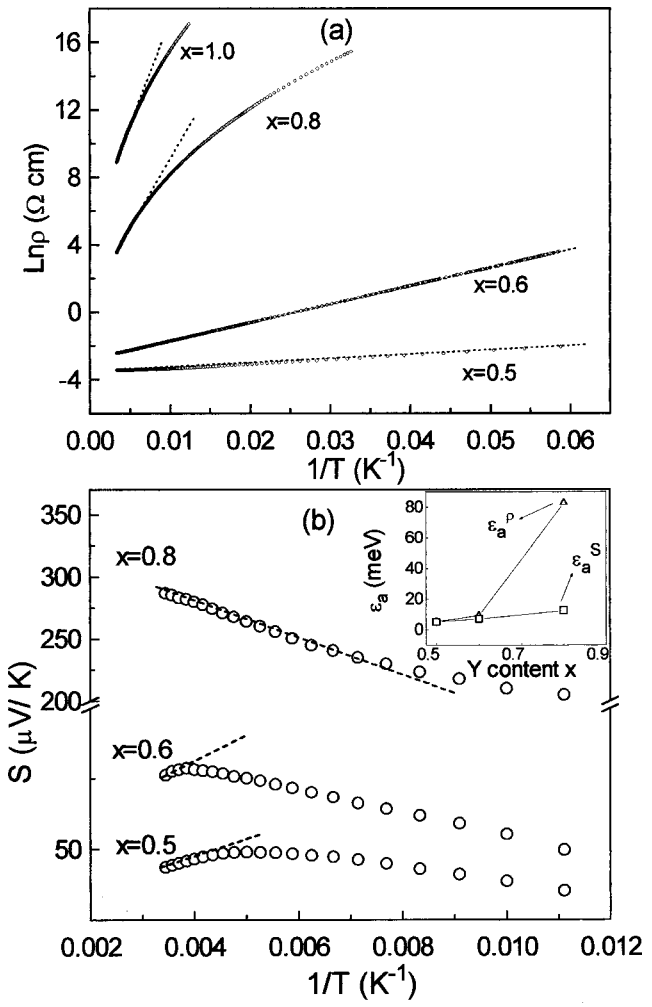

FIG. 7. (a) Resistivity in logarithmic scale vs $1/T$ for samples $Bi_2Sr_2Ca_{1-x}Y_xCu_2O_{8-\delta}$ ($x \geqslant 0.5$). (b) TEP vs $1/T$ for samples $Bi_2Sr_2Ca_{1-x}Y_xCu_2O_{8-\delta}$ ($x \geqslant 0.5$). The straight dashed lines are the linear fit at the high temperatures and give the thermal activation energy ε_a^ρ and ε_a^S in the inset (b).

dence. So it is suggested that the ESR signals mainly come from the localized Cu^{2+} spins.

Beschoten *et al.* studied the transport properties of $Bi_2Sr_2Ca_{1-z}Pr_zCu_2O_y$ and pointed out the coexistence of superconductivity and localization in the system.[32] The samples with low hole density have $d\mu^{-1}(T)/dT < 0$, which indicates hopping transport between localized states. For the $Bi_2Sr_2Ca_{1-x}Y_xCu_2O_{8-\delta}$ system, a semiconductinglike transport behavior can be clearly observed. To examine the possibility of polaron transport in this system, we compare the thermal activation energy derived from resistivity with that from TEP. One knows that for a thermally activated conduction process, the resistivity and TEP would show the following temperature dependence, respectively,

$$\rho(T) = \rho_0 \exp(\varepsilon_a / kT) \quad \text{and} \quad S(T) = \pm (k/e)(\varepsilon_a / kT + A),$$

where the + and − signs hold for hole-type and electron-type of conduction, and the constant A is determined by the energy dependence of the scattering time. In terms of the above equation, we plotted $\ln(\rho)$ and S as a function of $1/T$ for $Bi_2Sr_2Ca_{1-x}Y_xCu_2O_{8-\delta}$ samples in Figs. 7(a) and 7(b). The activation energy ε_a derived from the slope of straight lines at high temperature is shown in the inset of Fig. 7(b). Here we use ε_a^ρ and ε_a^S to denote the activation energy derived from resistivity and TEP, respectively. From the inset of Fig. 7(b) one can see that for $x \leqslant 0.6$ the value of ε_a^ρ and ε_a^S is close. But for $x > 0.6$ a large difference between ε_a^ρ and ε_a^S exists; i.e., $\varepsilon_a^\rho - \varepsilon_a^S$ is 70 meV for the sample with $x = 0.8$. Due to the TEP for the $x = 1.0$ sample not being obtained, we cannot further examine the change of activation energy. The discrepancy of ε_a^ρ and ε_a^S can be understood in terms of the small polaron model. So-called small polarons are the self-localized states, which are induced by the magnetic coupling between magnetic ions and hole spins.[33–35] From the small polaron model, it can be deduced that the polaron formation energy ε_p is twice as much as the difference between ε_a^ρ and ε_a^S; i.e., for the sample with $x = 0.8$, the polaron formation energy $\varepsilon_p = 2(\varepsilon_a^\rho - \varepsilon_a^S) = 140$ meV. This value is smaller than 204, 221, and 220 meV observed in $La_{2/3}Ca_{1/3}MnO_3$,[36] $La_{1.05}Sr_{0.95}Cu_{0.2}Co_{0.8}O_y$,[37] and $La_{1.85}Sr_{0.15}Cu_{1-x}Ni_xO_4$,[38] respectively, but it is larger than 60 meV determined by optical conducting measurements for $La_{1.85}Sr_{0.15}CuO_{4+\delta}$. It has been suggested that the formation energy of polarons is closely related to the size of the polaron. The polaron generally tends to expand with the reduction of formation energy. For example, for $La_{1.85}Sr_{0.15}CuO_{4+\delta}$ the ε_p is 60 meV, which is only a one-quarter of the ε_p (240 meV) (Ref. 34) in $La_{1.85}Sr_{0.15}NiO_4$; however, the polaron size of the former is almost 10 times as much as the latter. From this suggestion we can speculate that for the samples $Bi_2Sr_2Ca_{1-x}Y_xCu_2O_{8-\delta}$ with $x > 0.6$ small polarons gradually form and polaron transport plays a marked role in the normal-state transport.

We now turn our attention to the change of the T_m in the $S(T)$-T curve of the $Bi_2Sr_2Ca_{1-x}Y_xCu_2O_{8-\delta}$ system. One can clearly find in Fig. 5 that with Y doping the temperature (T_m) increases monotonously. Concerning the origin of the broad peak in the $S(T)$-T curve, many models have been proposed. For the non-electron-phonon interaction models, such as the spin-fluctuation,[39] spin bag,[40] Nagaosa-Lee,[41] and resonant-valence-bond (RVB) (Ref. 42) models, the characteristic energy that replaces the Debye energy is a low-lying magnetic excitation, which means that the TEP is field dependent. However, the results reported by Yu *et al.*[43] indicated that the TEP is independence of the magnetic field up to 30 T. This experiment cast doubt on magnetic models that utilize magnetic excitation as a characteristic energy. The electron-phonon interaction model is very successful in the application to normal metals or alloys. However, it has difficulty accounting for the transport data of high-T_c copper oxide superconductors, because of the low Debye temperature. It is noted that although the characteristic energy of the coupling of electron to acoustic phonon is low, the energies for optical-mode vibrations are high enough to yield a $T_m = 140$ K or higher. The vibronic coupling of electrons to optical-mode lattice vibrations proposed by Zhou and Goodenough[4] can be used to account for the transport data of most high-T_c copper oxide superconductors. And yet this model cannot be used to interpret the transport data involved strong spin scattering or local magnetic scattering, because it completely

ignores the magnetic interaction. We have investigated the transport properties of $La_{1.85-x}Sr_{0.15+x}Cu_{1-x}Fe_xO_4$ and $La_{1.85-x}Sr_{0.15+x}Cu_{1-x}Ga_xO_4$ systems, and found that Fe doping leads to the broad peak in $S(T)$-T curves shifting up from 100 to 200 K as the x increases from 0 to 0.13, while for the Ga doping system the temperature (T_m) is nearly unchanged.[5] Moreover, the double doping in both systems basically keeps a constant carrier concentration and the room-temperature TEP (S_{298}) between the two systems is very close. Based on these results, it is suggested that the localized magnetic scattering demonstrates a marked influence on the TEP. In the $Bi_2Sr_{2-x}CuO_6$ system we also observed that the localized Cu^{2+} spin scattering not only leads to a rapid increase in the resistivity, but also causes the bread peak in the S-T curve shifting to high temperature.[44] Therefore, for the above Y-doped Bi2212 system the increase of T_m should mainly originate from the localized Cu^{2+} spin scattering.

V. CONCLUSION

Experimental results show that Y doping causes a tetragonal-orthorhombic structural transition at $x=0.5$. The incommensurate modulation wavelength (q_b) varies from $4.8b$ for $x=0$ to $3.85b$ for $x=1.0$. The strongly structural distortion of the CuO_6 octahedron causes an increase of the fraction of localized Cu^{2+} spins, especially as $x \geqslant 0.6$, and the Cu3d electrons change from a partially delocalized to a localized state. The anomaly of transport properties around $x=0.6$ can be understood in terms of the change of spin correlation. A close relation between localized Cu^{2+} spin scattering and T_m is also proposed.

ACKNOWLEDGMENT

This work was supported by the Youth Foundation of the University of Science and Technology of China.

[1] G. Shirane, Y. Endoh, R. Birgeneau, M. A. Kastner, Y. Hidaka, M. Oda, M. Suzuki, and T. Murakami, Phys. Rev. Lett. **59**, 1613 (1987).
[2] T. Ito, K. Takenaka, and S. Uchida, Phys. Rev. Lett. **70**, 3995 (1993).
[3] Xu Gaojie, Mao Zhiqiang, Wu Wenbin, and Zhang Yuheng, J. Supercond. **10**, 555 (1997).
[4] J. S. Zhou and J. B. Goodenough, Phys. Rev. B **51**, 3104 (1995).
[5] Xu Gaojie, Mao Zhiqiang, Jin Hao, Yan Hongjie, and Zhang Yuheng, Phys. Lett. A **249**, 153 (1998).
[6] D. Mandrus, L. Forro, C. Kendziora, and L. Mihaly, Phys. Rev. B **44**, 2418 (1991).
[7] J. B. Mandal, S. Keshri, P. Mandal, A. Poddar, A. N. Das, and B. Ghosh, Phys. Rev. B **46**, 11 840 (1992).
[8] P. Sumana Prabhu, M. S. Ramachandra Rao, U. V. Varadaraju, and G. V. Subba Rao, Phys. Rev. B **50**, 6929 (1994).
[9] X. H. Chen, M. Yu, G. G. Qian, Z. S. Liu, L. Z. Cao, J. Zou, and C. Y. Xu, Phys. Rev. B **57**, 5082 (1998).
[10] A. Maeda, M. Hase, T. Sukada, K. Noda, S. TakeBayashi, and K. Uchinokura, Phys. Rev. B **41**, 6418 (1990).
[11] D. B. Mitzi, L. W. Lombardo, A. Kapitulnik, S. S. Laderman, and R. D. Jacowitz, Phys. Rev. B **41**, 6564 (1990).
[12] P. Mandal, A. Poddar, B. Ghosh, and P. Choudhury, Phys. Rev. B **43**, 13 102 (1991).
[13] M. Kakihana, M. Osada, M. Käll, L. Börjesson, H. Mazaki, H. Yasuoka, M. Yashima, and M. Yoshimura, Phys. Rev. B **53**, 11 796 (1996).
[14] T. W. Shaw and S. A. Shivashankar, Phys. Rev. B **37**, 9856 (1988).
[15] H. W. Zandbergen and W. A. Groen, Solid State Commun. **66**, 397 (1988).
[16] W. A. Groen, D. M. Deleeuw, and L. F. Feiner, Physica C **165**, 55 (1990).
[17] K. Tagaya, N. Fukuoka, and S. Nakanishi, Jpn. J. Appl. Phys., Part 1 **29**, 868 (1990).
[18] Y. Hayashi, M. Fukui, H. Sasakura, S. Minamigawa, T. Fujita, and K. Nakahigashi, Jpn. J. Appl. Phys., Part 1 **28**, 759 (1989).
[19] I. Ishida, K. Koga, S. Nakamura, Y. Lye, K. Kanoda, S. Okui, T. Takahashi, T. Oashi, and K. Kumagai, Physica C **176**, 24 (1991).
[20] H. W. Zandbergen, W. A. Groen, F. C. Mijhoff, G. Tendeloo, and S. Amelinckx, Physica C **156**, 325 (1988).
[21] Mao Zhiqiang, Fan Chenggao, Shi Lei, Yao Zhen, Yang Li, Wang Yu, and Zhang Yuheng, Phys. Rev. B **47**, 14 467 (1993).
[22] S. Amelinckx and G. Van Tendeloo, Physica C **235–240**, 162 (1994).
[23] Mao Zhiqiang, Zhang Hongguang, Tian Mingliang, and Zhang Yuheng, Phys. Rev. B **48**, 16 135 (1993).
[24] W. A. Groen and H. W. Zandbergen, Solid State Commun. **68**, 527 (1988).
[25] W. Bauhofer, H. Mattausch, R. K. Kremer, P. Murugaraj, and A. Simon, Phys. Rev. B **39**, 7244 (1989).
[26] M. Kakihana, L. Börjesson, C. Eriksson, P. Svedlindh, and P. Norling, Phys. Rev. B **40**, 6787 (1989).
[27] J. D. Jorgensen, B. W. Veal, A. P. Paulikas, L. J. Nowicki, G. W. Grabtree, H. Claus, and W. K. Kwok, Phys. Rev. B **41**, 1863 (1990).
[28] A. Manthiram and J. B. Goodenough, Appl. Phys. Lett. **53**, 420 (1988).
[29] M. Karppinen, A. Fukuoka, J. Wang, S. Takano, M. Wakata, T. Ikemachi, and H. Yamauchi, Physica C **208**, 130 (1993).
[30] Toshizo Fujita and Tsukasa Tomita, Physica C **162–164**, 985 (1989).
[31] B. I. Kochelaev, J. Sichelschmidt, B. Elschner, W. Lemor, and A. Loidl, Phys. Rev. Lett. **79**, 4274 (1997).
[32] B. Beschoten, S. Sadewasser, and G. Güntherodt, Phys. Rev. Lett. **77**, 1837 (1996).
[33] V. I. Anisimov, M. A. Korotin, J. Zaanen, and O. K. Andersen, Phys. Rev. Lett. **68**, 345 (1992).
[34] X.-X. Bi and P. C. Eklund, Phys. Rev. Lett. **70**, 2625 (1993).
[35] S-W. Cheong, H. Y. Hwang, C. H. Chen, B. Batlogg, L. W. Rupp, Jr., and S. A. Carter, Phys. Rev. B **49**, 7088 (1994).
[36] R. Muhlstroh and H. G. Reik, Phys. Rev. **162**, 703 (1967).
[37] Xu Gaojie, Mao Zhiqiang, Jin Hao, Yan Hongjie, Wang Bin, and Zhang Yuheng, Phys. Rev. B **59**, 12 090 (1999).
[38] Mao Zhiqiang, Xu Gaojie, Wang Bin, Yan Hongjie, Qiu Xueyin, and Zhang Yuheng, Phys. Rev. B **58**, 15 116 (1998).

[39] A. J. Millis, H. Monien, and D. Pines, Phys. Rev. B **42**, 167 (1990).
[40] J. R. Schrieffer, X. G. Wen, and S. C. Zhang, Phys. Rev. Lett. **60**, 944 (1988); Phys. Rev. B **39**, 11 663 (1989).
[41] N. Nagaosa and P. A. Lee, Phys. Rev. Lett. **64**, 2450 (1990).
[42] P. W. Anderson, Science **215**, 1196 (1987).
[43] R. C. Yu, M. J. Naughton, X. Yan, and P. M. Chaikin, Phys. Rev. B **37**, 7963 (1988).
[44] Xu Gaojie, Mao Zhiqiang, Yan Hongjie, and Zhang Yuheng, J. Phys.: Condens. Matter **10**, 8843 (1998).